Available online at www.sciencedirect.com
SCIENCE DIRECT
Journal of Molecular Catalysis A: Chemical 244 (2006) 229–236
JOURNAL OF MOLECULAR CATALYSIS A: CHEMICAL
www.elsevier.com/locate/molcata

Identification of Mo active species for methane dehydro-aromatization over Mo/HZSM-5 catalysts in the absence of oxygen: ^{1}H MAS NMR and EPR investigations

Hongmei Liu, Wenjie Shen, Xinhe Bao, Yide Xu *

State Key Laboratory of Catalysis, Dalian Institute of Chemical Physics, Chinese Academy of Sciences, 457 Zhongshan Road, P.O. Box 110, Dalian 116023, China

Received 23 June 2005; received in revised form 9 September 2005; accepted 9 September 2005
Available online 17 October 2005

Abstract

The effect of pre-reduction with H_2 at a low temperature, i.e. 623 K, on the structure of the Mo/HZSM-5 catalyst prepared by impregnation has been studied and characterized by means of ^{1}H MAS NMR and EPR techniques. It has been revealed that there are three kinds of Mo species on the Mo/HZSM-5 catalyst, namely, the $Mo_{6c}{}^{6+}$ oxide species with distorted octahedral coordination, the $Mo_{5c}{}^{6+}$ oxide species with square pyramidal coordination, and the Mo^{6+} oxide species associated with the Brönsted acid sites. The first two Mo oxide species exist mainly on the external surface of the HZSM-5 zeolite, and can be readily reduced to form the β-Mo_2C species, while the last one resides primarily in the channels, and is difficult to be fully reduced to form Mo carbide species. The Mo oxide species associated with the Brönsted acid sites can be partially reduced to the MoO_xC_y species during the induction period, which play a crucial role in the methane dehydro-aromatization (MDA) reaction. The MoO_xC_y species with face centered cubic (fcc) structure are more active and more selective towards benzene, yet more stable than those Mo carbide species with hexagonally close packed (hcp) structure. It is likely that pre-reduction with H_2 at 623 K can enhance the topotactic transformation of the Mo specie from the hcp structure into the fcc structure, thus can improve greatly the catalytic activity and selectivity towards mono-aromatics, as well as the stability of the Mo/HZSM-5 catalyst.

Keywords: Methane; Aromatization; ZSM-5; Molybdenum; Pre-reduction; EPR

1. Introduction

Considerable attention has been focused on the transformation of natural gas (mostly methane) into highly value-added liquid fuels and petrochemicals, owing to the increasing consumption and the shortage of oil resources. Therefore, developing of more economic processes for methane conversion becomes one of the serious challenges facing catalytic chemists around the world [1]. Catalytic dehydrogenation and aromatization of methane in the absence of gas-phase oxygen into highly value-added chemicals such as benzene and naphthalene turn out to be a promising route for the effective utilization of natural gas [2–6]. Methane dehydroaromatization (MDA) occurs at relatively lower temperatures (about 1000 K), as compared with the homogeneous pyrolysis of methane. Recently, this reaction has been widely investigated, and various transition metal ions such as Mo, W, Re, V, Ga and Cr, as well as different zeolites such as HZSM-5, HZSM-11, HZSM-8, HMCM-41, HMCM-22, HMCM-49, H-beta, HY and H-mordenite, have been tested [7–15]. Up to now, however, the Mo/HZSM-5 catalyst is still regarded as the best one among the tested catalysts at a reaction temperature of 973 K and a methane space velocity of around 1500 ml/g h [16]. It is generally accepted that the Mo oxide species are well dispersed on/in the HZSM-5 zeolite after calcination, and the Mo species are reduced by CH_4 in the initial period of the reaction to form Mo carbide species, which are responsible for methane activation and for the formation of C_2H_y species ($y < 4$) [17,18]. Moreover, due to the unique channel structure of the HZSM-5, together with its Brönsted acid sites and the suitable pore size of 0.53 nm × 0.56 nm, which is close to the kinetic diameter of benzene molecule, aromatization of the C_2 intermediates can proceed easily [15,19].

* Corresponding author. Tel.: +86 411 84379189(O); fax: +86 411 84694447.
E-mail address: xuyd@dicp.ac.cn (Y. Xu).

1381-1169/$ – see front matter © 2005 Elsevier B.V. All rights reserved.
doi:10.1016/j.molcata.2005.09.006

There are several kinds of Mo species in different states and various coordination environments on/in the Mo/HZSM-5 catalysts, as identified by FT-IR, ISS, NH_3-TPD [7,18,20], NH_4OH extraction and ^{27}Al, ^{29}Si MAS NMR techniques [21,22]. Usually, the Mo oxide species are highly dispersed on the HZSM-5 surface, and interact with the Brönsted acid sites of the HZSM-5 if the Mo loading is less than 8 wt%, and the calcination temperature is lower than 823 K. With an increasing Mo loading, MoO_3 crystallites can be detected by XRD and FT-IR [7]. On the other hand, the extraction of framework Al by the Mo oxide species will become more severe with the increase of the Mo loading and the calcination temperature. Up to now, what kind of Mo oxide species are acting as the precursor of the active Mo carbide species in MDA is still under discussion. Lunsford et al. and Solymosi et al. suggested that the Mo_2C species, highly dispersed on the external surface of the HZSM-5 zeolite, played the role of active sites and were responsible for initial methane activation [23–27]. Iglesia et al. demonstrated that most of the Mo species could migrate into the channels, replacing the Brönsted acid sites and anchoring on them [28–31]. Recently, they have used silicon-containing organic molecules to selectively interact with the external Brönsted acid sites of the HZSM-5 zeolite (so called silanation method), which could lead to residence of all Mo species in the channels. The Mo/HZSM-5 catalyst prepared by using the zeolite modified by silanation method exhibited excellent performances in the MDA. The authors also showed that the Mo species in the channels were less sensitive in forming carbonaceous deposits, and were more effective for methane activation [19]. Our previous studies revealed that the reducibilities of the Mo species located at various positions on/in the HZSM-5 zeolite were different, i.e. the MoO_x species which were non-associative with the Brönsted acid sites could be easily and fully reduced into the Mo carbide species by methane, whilst the Mo species associating with the Brönsted acid sites could only be partially reduced by CH_4, which, very likely, formed the MoO_xC_y species [32].

Many kinds of Mo carbide species can be formed, depending on the nature of the Mo precursors and the carburization conditions, as has been reported in [33–35]. Recently, Derouane-Abd Hamid and co-workers have studied the effect of different phases of the Mo carbide species phases on the catalytic performance of the Mo/HZSM-5 catalysts in MDA. They have found that if the Mo/HZSM-5 catalyst was pre-reduced with a mixture of n-C_4H_{10}/H_2 at 623 K for 24 h and then reacted with CH_4, the catalyst was more active and stable for the MDA reaction. The authors claimed that the Mo carbide species thus formed after prereduction with a mixture of n-C_4H_{10}/H_2 at 623 K for 24 h was in the form of α-MoC_{1-x}, which was a face centered cubic (fcc) structure. On the other hand, most of the studies reported in the literature concluded that the Mo carbide species of the Mo/HZSM-5 catalysts were in the form of β-Mo_2C with a hexagonally close packed (hcp) structure [36–38].

In this work, the effects of hydrogen prereduction at a low temperature (623 K) on the structure as well as the catalytic performances for MDA of a 6 wt% Mo/HZSM-5 catalyst were investigated by ^1H MAS NMR and EPR techniques. EPR was used to monitor and characterize the alteration in chemical environment and coordination of the Mo species during the prereduction and the early reaction stages, while the ^1H MAS NMR technique was used to monitor the changes of various hydroxyl groups on the HZSM-5 zeolite during the preparation and prereduction stages of the Mo/HZSM-5 catalysts.

2. Experimental

2.1. Catalyst preparation

The Mo/HZSM-5 catalyst having a Mo loading of 6 wt% was prepared by the conventional impregnation method. In brief, a HZSM-5 zeolite (supplied by Nankai University, $SiO_2/Al_2O_3 = 50$) was impregnated with an aqueous solution containing the desirable amount of ammonia heptamolybdate ($(NH_4)_6[Mo_7O_{24}]\cdot 4H_2O$), and then dried at room temperature for 12 h. Finally, it was dried at 393 K for 2 h and calcined in air at 773 K for 6 h. For use as samples of catalyst evaluation and characterization, the catalyst was crushed and sieved to 250–425 μm granules (20–60 mesh).

2.2. Catalyst activation via prereduction

Before reaction, the Mo/HZSM-5 catalyst was prereduced in situ by H_2. A catalyst sample (0.2 g) was charged into a fixed-bed quartz tubular reactor of 6.2 mm I.D, and a hydrogen flow of 2400 ml/(g cat h) was introduced into the reactor. After H_2-prereduction, a 10% N_2/CH_4 stream (1500 ml/g cat h) was switched into the reactor and the temperature was raised to 973 K at a heating rate of 5 K/min. All gases used in this work were of UHP grade and were used without further purification. The catalyst, prereduced with H_2, was denoted as Mo/HZSM-5(H), while that without H_2-prereduction and was directly heated in a 10% N_2/CH_4 stream to the reaction temperature of 973 K, was denoted as Mo/HZSM-5(O).

2.3. Catalytic test

After the H_2-prereduction, the catalyst was evaluated in a fixed-bed flow reactor at 973 K and atmospheric pressure. The catalyst charge was 0.2 g. The feed was a gas mixture of 10% N_2/CH_4 (1500 ml/(g cat h)), and the N_2 in the CH_4 was used as an internal standard, as reported by Lunsford et al. [18], for measuring the CH_4 conversion as well as the selectivity of all products and carbonaceous deposits. On-line analysis of the effluent was performed with a Hewlett-Packard 6890 gas chromatograph. The hydrocarbon products, including ethane, ethylene and condensable C_6–C_{10} aromatics such as benzene, toluene, xylene and naphthalene, etc., were separated by using a methyl-silicone HP-1 capillary column (0.32 mm × 50 m) and determined by a flame ionization detector (FID). For on-line separation and analysis of H_2, N_2, CO, CH_4, CO_2, C_2H_4 and C_2H_6, etc., a HayeSep-D column (3 mm × 2 m) and a thermal conductive detector (TCD) were equipped on the same gas chromatograph. Methane conversion, selectivity of hydrocarbon products, and coke formation were evaluated according to carbon mass balance. All reaction

rates were calculated basing on carbon balance and expressed as mmoles per gram of catalyst per second.

2.4. Catalyst characterization

^{1}H MAS NMR experiments were carried out at 400.1 MHz on a Bruker DRX-400 spectrometer with a BBI MAS probe and 4 mm ZrO_2 rotors. Prior to the experiments, the Mo/HZSM-5 catalyst sample was pretreated in two different ways. In one case, the sample was dehydrated in a He stream at 623 K for 20 h to remove adsorbed water. In the other case, the sample was first reduced by hydrogen (2400 ml/g cat h) at 623 K for 6 h and then dehydrated in a He flow at 623 K for 20 h. After the pretreatment, the sample was put into the NMR rotor for measurement without exposing to air. Each sample was spun at 8 kHz, and 200 scans were accumulated. Chemical shifts were referenced to a saturated aqueous solution of 4,4-dimethyl-4-silapentane sulfonate sodium (DSS). The number of Brönsted acid sites per unit cell in the parent zeolite was calculated from the corresponding unit cell composition. The number of Brönsted acid sites per unit cell of the Mo/HZSM-5 catalyst after calcination was estimated by comparing the peak areas of the ^{1}H MAS NMR spectra with the corresponding parent zeolite.

All EPR experiments were performed on a JEOL ES-EO3X X-band spectrometer at room temperature. A microwave frequency γ of 9.42 GHz and a power of 1 mw were used. The relative spin concentration and the g factor were calculated by taking the signal of manganese as an internal standard. A specially designed EPR flow reactor cell was employed, which could be placed in the resonance cavity. The reactor cell for EPR measurement was made of quartz (4 mm I.D.,) and was nomally charged with 0.2 g of catalyst sample. With this reactor cell, the real fix-bed catalytic reaction could be simulated. After the reaction or prereduction, the reactor was transferred into the resonance cavity of the EPR spectrometer under a protecting gas. The EPR spectra were digitized and doubly integrated by the PEAKFIT workstation in order to calculate the relative spin concentration. The Mo/HZSM-5 catalyst sample was prereduced with H_2 (2400 ml/g cat h) at 623 K for 6 h. Then a methane stream (1500 ml/g cat h) was introduced into the reactor cell, and the temperature was increased to 973 K. The EPR signals were recorded during the processes of H_2-pretreatment and methane treatment, respectively.

3. Results and discussion

3.1. Effect of H_2-prereduction conditions of Mo/HZSM-5 on the catalytic performances of MDA

The catalytic performances of MDA over 6Mo/HZSM-5(H) catalysts prereduced with H_2 at different temperatures for 6 h were investigated and the results were compared with those of a non-prereduced 6Mo/HZSM-5(O) catalyst. Fig. 1 shows the methane depletion rate and the BTX formation rate over these catalysts after running the reaction for 24 h. Over the 6Mo/HZSM-5(O) catalyst, the rate of methane depletion was 1.2×10^{-3} mmol/g cat-s, and the rate of BTX formation was

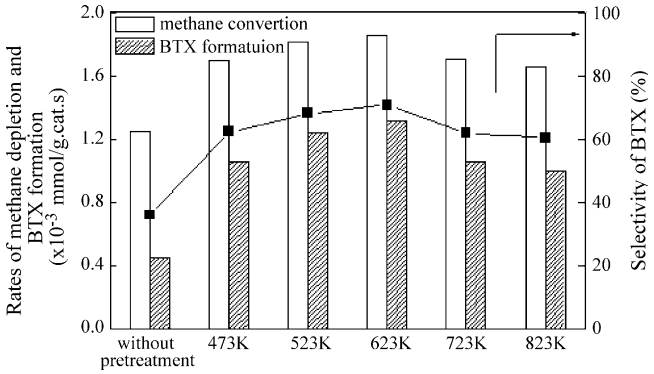

Fig. 1. Rates of methane depletion and BTX formation, as well as BTX selectivity on 6Mo/HZSM-5(O) and 6Mo/HZSM-5(H) catalysts (prereduced with H_2 at different temperatures) after 24 h time-on-stream for MDA (973 K, 1 atm, GHSV: 1500 ml/(g cat h), H_2-prereduction time: 6 h).

0.4×10^{-3} mmol/g cat-s. After the 6Mo/HZSM-5 catalyst was prereduced with H_2 for 6 h at different temperatures, its catalytic performance was improved. The methane conversion and the BTX formation over the 6Mo/HZSM-5(H) catalyst both increased with the increasing of the prereduction temperature, and reached its highest value at the prereduction temperature of 623 K. Then they went down with a further rising of the H_2-prereduction temperature from 623 to 823 K, as shown in Fig. 1. Meanwhile, the effect of prereduction temperature on the product distribution of MDA over the 6Mo/HZSM-5(H) catalysts was quite apparent. On the 6Mo/HZSM-5(H) catalyst which was prereduced with H_2 at 623 K for 6 h, the BTX selectivity was about 71%, as compared with that of about 36% on the 6Mo/HZSM-5(O) catalyst. It is clear that 623 K is a proper temperature for H_2-prereduction to obtain the best MDA performance over the Mo/HZSM-5(H) catalyst.

The performance of the 6Mo/HZSM-5(H) catalyst could also be affected by the pretreduction time, and the best prereduction time has been found to be about 6 h, as shown in Fig. 2. No further enhancement could be observed with a further prolonging of the prereduction time.

Thus, it can be concluded that prereduction with H_2 at 623 K for 6 h is the most appropriate treatment condition in allowing the 6Mo/HZSM-5 catalyst to exhibit its best catalytic perfor-

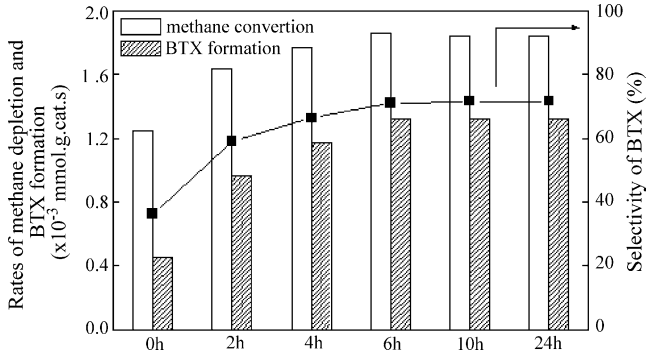

Fig. 2. Rates of methane depletion and BTX formation, as well as BTX selectivity on 6Mo/HZSM-5(O) and 6Mo/HZSM-5(H) catalysts (prereduced with H_2 for various durations of time) after 24 h time-on-stream for MDA (973 K, 1 atm, GHSV: 1500 ml/(g cat h), H_2-prereduction temperature: 623 K).

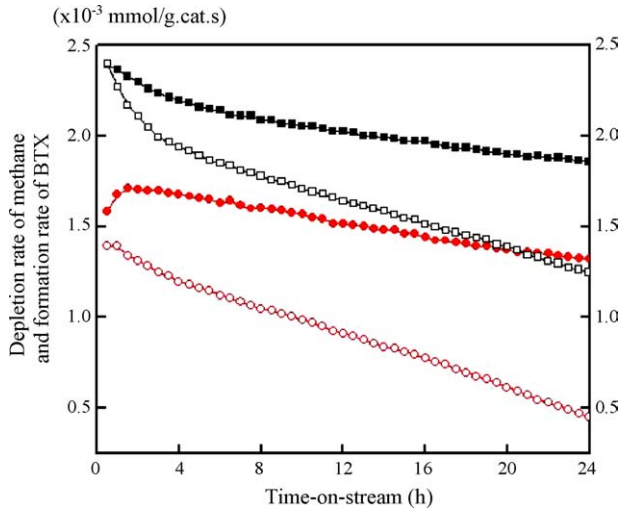

Fig. 3. Dependence of rates of methane depletion (■) and BTX formation (●) over Mo/HZSM-5 catalysts on time on stream of MDA. Open symbols for the 6Mo/HZSM-5(O) catalyst. Solid symbols for the 6Mo/HZSM-5(H) catalyst pretreated in hydrogen at 623 K for 6 h.

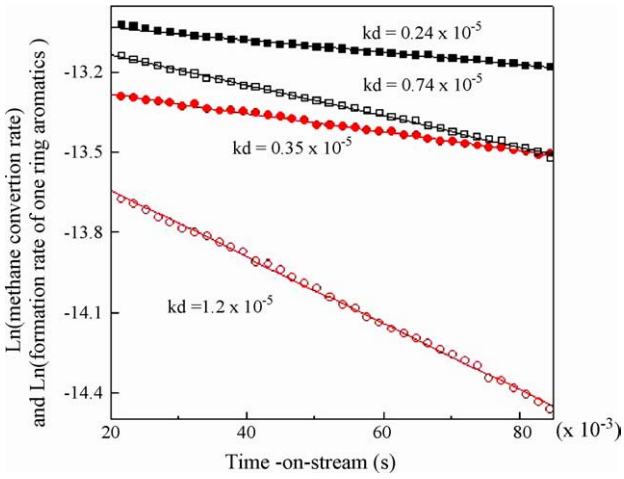

Fig. 4. Rates of methane depletion (■) and BTX formation (●) as a function of time on stream over 6Mo/HZSM-5 catalysts (the values of k_d are calculated from the slope of semilogarithmic plot). Open symbols for the 6Mo/HZSM-5(O) catalyst. Solid symbols for the 6Mo/HZSM-5(H) catalyst pretreated in hydrogen at 623 K for 6 h.

mance. Fig. 3 shows the rates of methane depletion and BTX (the main products) formation on the 6Mo/HZSM-5(O) catalyst and the 6Mo/HZSM-5(H) catalyst prereduced with H_2 at 623 K for 6 h. As illustrated in Fig. 4, the deactivation rate constant, k_d, of the depletion rate of methane over the 6Mo/HZSM-5(H) catalyst is $0.24 \times 10^{-5}\ s^{-1}$ for an on-stream time of 24 h, and the deactivation rate constant for the formation of BTX is about $0.35 \times 10^{-5}\ s^{-1}$, as compared with those of $0.74 \times 10^{-5}\ s^{-1}$ and $1.2 \times 10^{-5}\ s^{-1}$, respectively, over the 6Mo/HZSM-5(O) catalyst. Obviously, both the activity and the stability for methane conversion and aromatics formation over the 6Mo/HZSM-5 catalysts were greatly improved after prereduction with H_2 at 623 K for 6 h.

3.2. ^{1}H MAS NMR results

The parent HZSM-5 zeolite as well as the 6Mo/HZSM-5(O) and 6Mo/HZSM-5(H) catalysts were investigated by using the ^{1}H MAS NMR technique. There were five types of characteristic resonance lines appearing after the ^{1}H MAS NMR spectrum of the dehydrated parent HZSM-5 zeolite was deconvoluted, as reported previously in refs. [39–44]. The high-field signal with a chemical shift of 1.7 ppm can be ascribed to external Si-OH groups, while the second peak at $\delta = 2.4$ ppm is associated with extraframework Al–OH [39–42]. The low-field signal at $\delta = 3.8$ ppm belongs to the bridging OH groups in the form of free Al–OH–Si groups locating at the intersections of the channels of the zeolites, which are the so-called free Brönsted acid sites [39–43]. And the broad resonance peak at about 6.0 ppm can be due to another kind of Brönsted acid sites, termed as the restricted Brönsted acid sites, which are affected by additional electrostatic interaction of the oxygen atoms in the zeolite framework, as described in ref. [43]. In addition, the resonance signal of the water adsorbed on the Lewis acid sites exhibited a chemical shift of 4.7 ppm. [44]. Variation in the number of different kinds of hydroxyl groups per unit cell on the HZSM-5 zeolite and the two 6Mo/HZSM-5 catalysts are listed in Table 1. Obviously, introduction of the Mo species led to a significant decrease in all kinds of hydroxy groups, especially in Brönsted acid sites. Since the Brönsted acid sites of HZSM-5 zeolites are mainly located on the inter-surface, as reported by Bao and coworkers [45], the obvious decrease of the Brönsted acid sites indicates that the Mo species would first disperse on the surface of the HZSM-5 zeolite and then migrate into the channels to interact with and replace the Brönsted acid sites.

It is interesting to notice that the spectra of the 6Mo/HZSM-5(O) and 6Mo/HZSM-5(H) catalysts are almost the same. Only a few changes could be observed in the number of different kinds of OH groups (i.e. external Si–OH groups, extraframework Al–OH groups and Brönsted acid sites) after the 6Mo/HZSM-5

Table 1
Numerical results of ^{1}H MAS NMR experiments on the parent HZSM-5 zeolite and 6Mo/HZSM-5 catalysts

Sample	The number of hydroxyls per unit cell					Number of B acid site per u.c.[a]
	B2 (6.0 ppm)	Water (4.7 ppm)	B1 (3.8 ppm)	Al–OH (2.3 ppm)	Si–OH (1.7 ppm)	
HZSM-5	1.9	1.9	2.1	0.50	0.54	4.0
6Mo/HZSM-5(O)	0.5	0.2	0.7	0.22	0.08	1.2
6Mo/HZSM-5(H)	0.5	0.1	0.7	0.23	0.07	1.2

[a]The number of Brönsted acid sites per unit cell = B1 + B2, the number of Brönsted acid sites per unit cell of the HZSM-5 zeolite was calculated from the unit cell formula on the basis of the Si/Al ratio, which is measured by ^{29}Si MAS NMR.

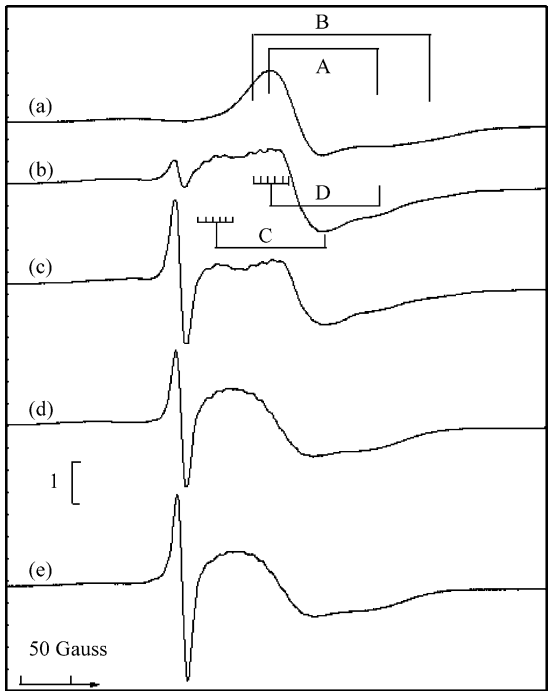

Fig. 5. EPR spectra of 6Mo/HZSM-5(H) catalyst after prereduced with H_2 at 623 K for 6 h (a), and after running the MDA for 0.5 h (b), 1 h (c), 2 h (d) and 4 h (e) at 973 K.

catalyst was prereduced with H_2 at 623 K for 6 h. Neither changes in dispersion of the Mo species on the external surface nor in the amount of Mo species migrating into the channels of HZSM-5 zeolite was caused by the H_2-prereduction process.

3.3. EPR results

EPR is a sensitive technique for monitoring variations in the chemical environment and coordination sphere of paramagnetic species. The Mo oxide species on the Mo/HZSM-5 catalyst prepared by impregnation mainly exist in the form of Mo^{6+} after calcination at 773K, which is diamagnetic, so that no EPR signals could be observed at room temperature if the 6Mo/HZSM-5 catalyst had not been subjected to any further treatments (spectrum not show here). The EPR spectrum of the Mo species on the 6Mo/HZSM-5 catalyst after H_2-prereduction at 623 K for 6 h is shown in Fig. 5a. Two smooth and axially symmetric EPR signals appeared, but overlapping with each other. For simplification, the signals located at $g_\perp = 1.950$, $g_{||} = 1.894$ and $g_\perp = 1.959$, $g_{||} = 1.866$ were denoted as A and B, respectively. The shape and g values of the signals A and B are very similar to the EPR signals of the Mo^{5+} species formed on various supported molybdenum-based catalysts subjected to different reduction treatments, as reported previously in [46–50]. Che and co-workers suggested that both of the two Mo^{5+} species, corresponding to the signals A and B, possess a short Mo=O bond and are surrounded only by oxygen ligands. Signal A was attributed to $Mo_{6c}{}^{5+}$ species with a distorted octahedral coordination symmetry, and signal B to $Mo_{5c}{}^{5+}$ species in the form of square pyramidal coordination [49,50]. After the sample was prereduced with H_2 at 623 K, both of the signals corresponding to the $Mo_{6c}{}^{5+}$ and $Mo_{5c}{}^{5+}$ species appeared, indicating that the Mo^{6+} species can be reduced readily to Mo^{5+}, either in the form of compressed octahedral coordination or in a square pyramidal coordination. Xu and co-workers have reported that, when a 2 wt% Mo/HZSM-5 catalyst was reduced in a methane stream at 573 K for 1 h, the signals A and B could be well detected. The authors suggested that the $Mo_{6c}{}^{5+}$ and $Mo_{5c}{}^{5+}$ species existed mainly on the extra-surface of the HZSM-5 zeolite [32]. In addition, signal A is much more intense than signal B, as shown in Fig. 5a, implying that a large part of the Mo species located on the external surface is in distorted octahedral coordination.

After the 6Mo/HZSM-5 catalyst was prereduced in situ with H_2 at 623 K for 6 h, a methane stream (1500 ml/g cat h) was introduced into the reactor, and the temperature was raised to 973 K, which is the temperature for MDA. Fig. 5b–e shows the changes in EPR spectra with time on stream of the reaction. After running the MDA reaction for 0.5 h, the EPR spectrum was totally different from that recorded at the end of the H_2-prereduction. First, a new detectable isotropic signal located at $g = 2.003$ appeared. As suggested by Lange and co-workers, the appearance of this signal is due to the free electrons of condensed aromatics or graphite-like coke [51]. Thus, the appearance of this signal indicates the formation of carbonaceous deposits. With an increase of the time on stream from 0.5 to 1 h, an evident increase of the signal located at $g = 2.003$ (Fig. 5c) could be found, while the shape and the line width of the isotropic signal changed scarcely. Obviously, the increase in intensity was mainly resulted from the formation of the more carbonaceous deposits on the surface of the 6Mo/HZSM-5(H) catalyst. Second, the overall signal of the Mo^{5+} species became rather complicated. Signal B disappeared completely, indicating that there was a further reduction of the square-pyramidally coordinated $Mo_{5c}{}^{5+}$ species on the extra-surface of the HZSM-5 zeolite. On the other hand, a new six-line and axially symmetric signal, locating at $g_\perp = 1.983$ $g_{||} = 1.921$ and denoted as signal C, appeared, which contributed mainly to the overall Mo^{5+} signal. It is clear that signal C represents superimposed hyperfine structures, and the splitting of the $g_{||}$ is not so severe as the splitting of the $g_\perp$. Such kinds of splitting lines in the EPR spectra of Mo/HZSM-5 catalysts have been reported only in ref. [32]. The authors suggested that the splitting signal C should also be assigned to the Mo^{5+} species. The hyperfine structure (HFS) of this signal are resulted from the existence of the nearby odd nucleus moment, when the Mo^{5+} species are located at positions closely associated with the framework ^{27}Al species ($I = 5/2$). The super-hyperfine interaction between the Mo^{5+} species and the ^{27}Al atoms will lead to a splitting of the Mo^{5+} EPR signal. Therefore, the Mo species corresponding to the six-lined splitting signal C are proposed to be mononuclear Mo^{5+} cations having a particular interaction with the framework Al species and are located in the channels of the HZSM-5. This assignment is very similar to those reported in the cases of Cr/HZSM-5 and Cu/HZSM-5 [52–54]. Recently, two-dimensional ^{27}Al MAS NMR has been used to study the Al species on Mo/HZSM-5 catalysts prepared by impregnation, and the experimental results testified the existence of strong interaction between the Mo species and the framework Al atoms through Mo–O–Al bonds [55]. Results from ^{1}H MAS NMR

experiments suggested that the Mo species would migrate into the channels during thermal treatments, and would replace the Brönsted acid sites, thus resulting in a decrease in the number of Brönsted acid sites [56]. Therefore, it is reasonable to attribute the signal C to Mo species associated with the Brönsted acid sites, and most of them are residing inside the channels of the HZSM-5 zeolite. Signal C would not appear if the temperature of reduction with CH_4 was lower than 973 K, suggesting that the reduction of the Mo^{6+} species associated with the Brönsted acid sites to Mo^{5+} species are much more difficult than those of the Mo^{6+} species on the extra-surface of the HZSM-5 zeolite.

Moreover, signal A, locating at $g_{\perp} = 1.950$ and $g_{||} = 1.894$ and corresponding to the $Mo_{6c}{}^{5+}$ species in distorted octahedral coordination, changed significantly in shape, as compared to that in Fig. 5a. After treating the catalyst sample with a flow of methane at 973 K for 30 min, the $g_{\perp}$ tensor of this signal splitted, and showed the same HFS as in signal C. To simplify the discussion, signal A that exhibited six-lined spitting is denoted as signal D. The g tensors of signal D are almost the same as those of signal A, indicating that the distorted-octahedrally coordinated Mo^{5+} species locating at the external surface of the HZSM-5 zeolite would not change its coordination environment with respect to oxygen ligands. Meanwhile, the splitting in signal D suggests that the interaction between the Mo species and the parent zeolite was strengthened during the methane treatment. Probably, the unpaired electrons of the Mo species were affected by the Al atoms through the bridging oxygen.

Even though the intensity of the overall Mo^{5+} signal decreased, both the signals C and D could still be clearly observed. Moreover, it should be noted that, the decrease in intensity of signal D is larger than that of signal C. This implies that further reduction of the Mo^{5+} species on the extra-surface of the HZSM-5 is easier than the Mo^{5+} species associated with the Brönsted acid sites locating in the channels of the zeolite. With a further increasing of the reaction time from 1 to 2 h or from 2 to 4h, the intensities of the splitted signals C and D decreased continuously, particularly in the high field signal D (in Fig. 5d and e).

Fig. 6 shows the EPR spectra of the 6Mo/HZSM-5(O) catalyst after heating in methane at 973 K for various durations of time. The symmetrical signal, located at $g = 2.003$ and ascribed to the carbonaceous deposits, as well as the signal of the Mo^{5+} species, could be observed clearly after the 6Mo/HZSM-5(O) catalyst had been heated at 973 K in a CH_4 stream for 30 min. The overlapping signal for the Mo^{5+} species is mainly composed of the two signals of A and B. Meanwhile, a weak signal C could be detected, but the superimposed splitting structures of this signal were not easily distinguished. This suggests that all of the Mo^{6+} species on the Mo/HZSM-5 catalyst can be reduced to Mo^{5+} in a CH_4 flow at 973 K to form the $Mo_{6c}{}^{5+}$ and $Mo_{5c}{}^{5+}$ species which are located on the external surface of the HZSM-5, as well as to the Mo^{5+} species associated with the Brönsted acid sites. After the 6Mo/HZSM-5(O) catalyst was heated at 973 K in a CH_4 stream for 60 min, the intensity of signal C increased significantly, and the hyperfine structures of this signal became quite clear. These changes in signal C testify that more Mo species associated with the Brönsted acid sites were reduced

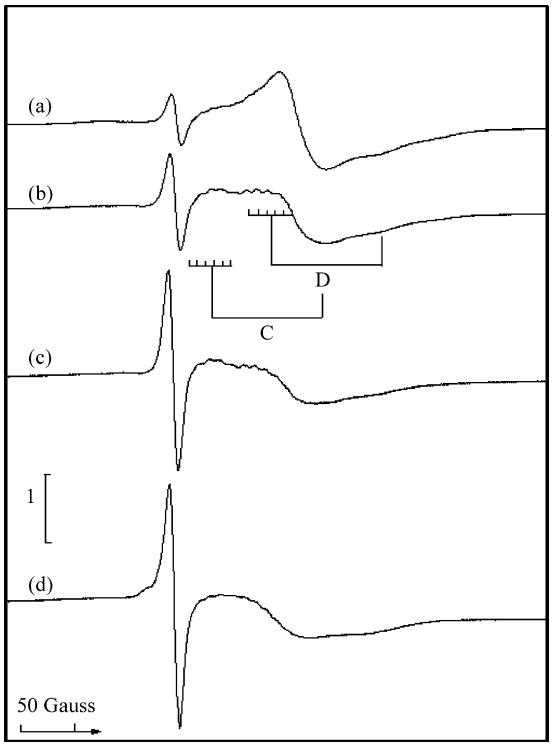

Fig. 6. EPR spectra of the 6Mo/HZSM-5(O) catalyst after running the MDA reaction for 0.5 h (a), 1 h (b), 2 h (c) and 4 h (d) at 973K.

to form Mo^{5+} species. Accompanying the decrease in intensity of signal B, signal A became a six-lined splitting structure of signal D. However, the intensity of signal D of the 6Mo/HZSM-5(O) sample was not so intense as that of the Mo/HZSM-5(H) sample. By extending further the treating time at 973K in the CH_4 stream, there were no distinct changes in the EPR spectra of the 6Mo/HZSM-5(O) catalyst, with only a continuous decrease in the intensity of the Mo^{5+} signal, especially in the high field signal C, accompanied by an continuous increase in the intensity of the coke signal.

The EPR results revealed that there are three kinds of Mo species on the Mo/HZSM-5 catalyst prepared by impregnation: the $Mo_{6c}{}^{5+}$ species in distorted octahedral coordination, the $Mo_{5c}{}^{6+}$ species in square pyramidal coordination, and the Mo^{6+} species associated with the Brönsted acid sites. The former two Mo species existed mainly on the external surface of the parent HZSM-5 zeolite and could be easily reduced to Mo^{5+}, while the latter one resided primarily inside the channels. Furthermore, during the MDA reaction at 973 K, there were two kinds of Mo^{5+} species present on the Mo/HZSM-5 catalyst, one was derived from the Mo_{6c} species interacting with the HZSM-5 zeolite, while the other was associated with the Brönsted acid sites. With the progressing of the reaction, a part of the Mo^{5+} species, mainly the Mo species on the external surface of the HZSM-5 zeolite, was further reduced by methane. The quantitative results of the EPR experiments are shown in Fig. 7 by double integrating the overall Mo^{5+} signal. It is evident that, the overall amount of the Mo^{5+} species (mainly corresponding to signals C and D) on the 6Mo/HZSM-5(H) is much larger than that on the 6Mo/HZSM-5(O) catalyst. ^{1}H MAS NMR results

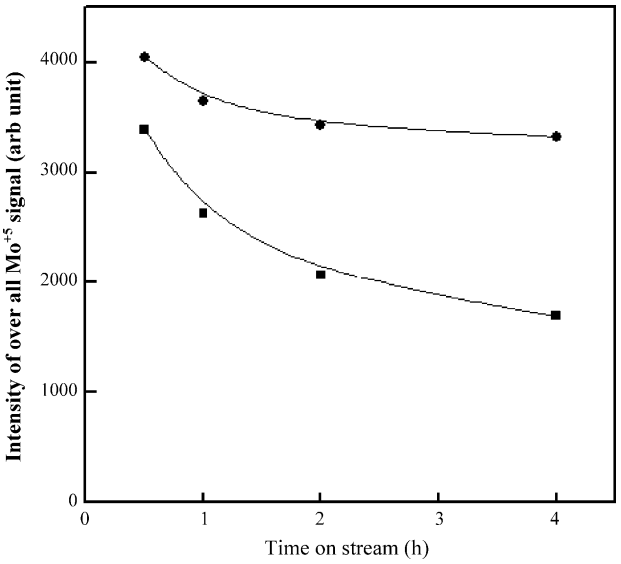

Fig. 7. The intensities of EPR signals of all Mo^{5+} species on the 6Mo/HZSM-5 (O) catalyst (■) and the 6Mo/HZSM-5 (H) catalyst (●).

also revealed that the number of all kinds of hydroxy groups on the 6Mo/HZSM-5 catalyst remained unchanged after the H_2-prereduction at 623 K. Therefore, further migration and dispersion of the Mo species on the external surface or into the channels of the HZSM-5 zeolite did not occur during the process of H_2-prereduction. It appears that the reduction of the Mo species with fcc structures is much more difficult than that of the Mo species with hcp structures, resulting in the amount of the Mo^{5+} species remaining on the 6Mo/HZSM-5(H) catalyst to be far higher than those on the 6Mo/HZSM-5(O) catalyst. Fig. 7 implies that partially reduced Mo carbide species may also play an important role in the MDA reaction.

Possibly, the difference in catalytic performance between the 6Mo/HZSM-5(O) and the 6Mo/HZSM-5(H) catalysts is due to that the MoO_xC_y species with fcc structure possess higher activity and better stability than those with hcp structure for the activation of methane and the formation of aromatics. If this speculation is true, the catalytic performance exhibited by the 6Mo/HZSM-5(H) catalysts prereduced with H_2 under various temperatures and durations of time can also be understood.

4. Conclusions

There are three kinds of Mo species on the Mo/HZSM-5 catalysts prepared by impregnation: the distorted octahedrally coordinated $Mo_{6c}{}^{6+}$ species, the square pyramidally coordinated $Mo_{5c}{}^{6+}$ species and the Mo^{6+} species associated with the Brönsted acid sites. The former two Mo species exist mainly on the external surface of the HZSM-5 zeolite, while the latter one resides primarily inside the channels. These Mo species can be reduced gradually in methane at 973 K into the β-Mo_2C/β-MoO_xC_y species with an hcp structure. On the other hand, prereduction of Mo/HZSM-5 with H_2 at 623 K for 6 h can lead to a topotactic transformation of the Mo species from the hcp to an fcc structure. The Mo species with an fcc structure are more difficult to be reduced by methane, as compared to the Mo species with an hcp structure. The Mo species with an fcc structure play a crucial role in the MDA reaction. This can give inspiration for creating a Mo/HZSM-5 catalyst with better activity for methane conversion, higher selectivity to aromatics and better catalytic stability.

Acknowledgments

Financial supports from the Ministry of Science and Technology of China under Contract G1999022406, and from the National Natural Science Foundation of China under grant No.20473086, as well as from the BP-CAS (China) Joint Center, are gratefully acknowledged.

References

[1] R.H. Crabtree, Chem. Rev. 95 (1995) 987.
[2] L. Wang, L. Tao, M. Xie, G. Xu, J. Huang, Y. Xu, Catal. Lett. 21 (1993) 35.
[3] Y. Xu, L. Lin, Appl. Catal. A 188 (1999) 53.
[4] J.H. Lunsford, Catal. Today 63 (2000) 165.
[5] Y. Shu, M. Ichikawa, Catal. Today 71 (2001) 55.
[6] Y. Xu, X. Bao, L. Lin, J. Catal. 216 (2003) 386.
[7] Y. Xu, S. Liu, L. Wang, M. Xie, X. Guo, Catal. Lett. 30 (1995) 135.
[8] Y. Shu, D. Ma, L. Xu, Y. Xu, X. Bao, Catal. Lett. 70 (2000) 67.
[9] Y. Shu, D. Ma, X. Liu, X. Han, Y. Xu, X. Bao, J. Phys. Chem. B 104 (2000) 8245.
[10] S. Liu, Q. Dong, R. Ohnishi, M. Ichikawa, Chem. Commun. (1997) 1455.
[11] L. Wang, R. Ohnishi, M. Ichikawa, J. Catal. 190 (2000) 276.
[12] J. Zeng, Z. Xiong, H. Zhang, G. Lin, K. Tsai, Catal. Lett. 53 (1998) 119.
[13] B.M. Weckhuysen, D. Wang, M.P. Rosynek, J.H. Lunsford, J. Catal. 175 (1998) 338.
[14] B.M. Weckhuysen, D. Wang, M.P. Rosynek, J.H. Lunsford, J. Catal. 175 (1998) 347.
[15] C. Zhang, S. Li, Y. Yuan, W. Zhang, T. Wu, L. Lin, Catal. Lett. 56 (1998) 207.
[16] Y. Shu, Y. Xu, S. Wong, L. Wang, X. Guo, J. Catal. 170 (1997) 11.
[17] F. Solymosi, J. Cserényi, A. Szöke, T. Bánsági, A. Oszkó, J. Catal. 165 (1997) 150.
[18] D. Wang, J.H. Lunsford, M.P. Rosynek, J. Catal. 169 (1997) 347.
[19] W. Ding, G. Meitzner, E. Iglesia, J. Catal. 206 (2002) 14.
[20] L. Chen, L. Lin, Z. Xu, X. Lian, T. Zhang, X. Li, J. Catal. 157 (1995) 190.
[21] W. Liu, Y. Xu, S. Wong, L. Wang, J. Qiu, N. Yang, J. Mol. Catal. A 120 (1997) 257.
[22] W. Liu, Y. Xu, J. Catal. 185 (1999) 386.
[23] D. Wang, J.H. Lunsford, M.P. Rosynek, Topics Catal. 3 (1996) 289.
[24] B.M. Weckhuysen, M.P. Rosynek, J.H. Lunsford, Catal. Lett. 52 (1998) 31.
[25] F. Solymosi, A. Erdohelyi, A. Szöke, Catal. Lett. 32 (1995) 43.
[26] A. Szöke, F. Solymosi, Appl. Catal. A 142 (1996) 361.
[27] F. Solymosi, A. Szöke, Catal. Lett. 39 (1996) 157.
[28] R.W. Borry III, Y.H. Kim, A. Huffsmith, J.A. Reimer, E. Iglesia, J. Phys. Chem. B 103 (1999) 5787.
[29] Y.H. Kim, R.W. Borry III, E. Iglesia, Micro. Meso. Mater. 35/36 (2000) 495.
[30] W. Li, G. Meitzner, R.W. Borry III, E. Iglesia, J. Catal. 191 (2000) 373.
[31] W. Ding, S. Li, G. Meitzner, E. Iglesia, J. Phys. Chem. B 105 (2001) 506.
[32] D. Ma, Y. Shu, X. Bao, Y. Xu, J. Catal. 189 (2000) 314.
[33] D.J. Sajkowski, S.T. Oyama, Appl. Catal. 134 (1996) 339.
[34] J.S. Lee, S.T. Oyama, M. Boudart, J. Catal. 106 (1987) 125.
[35] J.S. Lee, L. Volpe, F.H. Ribeiro, M. Boudart, J. Catal. 112 (1988) 44.

[36] C. Bouchy, S.B. Derouane-Abd Hamid, E.G. Derouane, Chem. Commun. 2 (2000) 125.
[37] S.B. Derouane-Abd Hamid, J.R. Anderson, I. Schmidt, C. Bouchy, C.J.H. Jacobsen, E.G. Derouane, Catal. Today 63 (2000) 461.
[38] C. Bouchy, I. Schmidt, J.R. Anderson, C.J.H. Jacobsen, E.G. Derouane, S.B. Derouane-Abd Hamid, J. Mol. Catal. A 163 (2000) 283.
[39] J. Klinowski, Chem. Rev. 91 (1991) 1459.
[40] L.W. Beck, J.L. White, J.F. Haw, J. Am. Chem. Soc. 116 (1994) 9657.
[41] M. Hunger, Catal. Rew. Sci. Eng. 39 (1997) 345.
[42] E. Brunner, H. Ernst, D. Freude, T. Frohlich, M. Hunger, H. Pfeiffer, J. Catal. 127 (1991) 34.
[43] M. Muller, G. Harvey, R. Pins, Micro. Meso. Mater. 34 (2000) 135.
[44] M. Hunger, D. Freude, H. Pfeifei, J. Chem. Soc. Faraday Trans. 87 (1991) 657.
[45] W. Zhang, X. Bao, X. Guo, X. Wang, Catal. Lett. 60 (1999) 89.
[46] R.F. Howe, I.R. Leith, J. Chem. Soc. Faraday Trans. 69 (1973) 1961.
[47] C. Louis, M. Che, J. Phys. Chem. 91 (1987) 2875.
[48] M.M. Huang, J.R. Johns, R.F. Howe, J. Phys. Chem. 92 (1988) 1291.
[49] M. Che, J.L. McAteer, A.J. Tench, J. Chem. Soc. Faraday Trans. 4 (1978) 2378.
[50] M. Che, M. Fournier, J.P. Launay, J. Phys. Chem. 71 (1979) 1954.
[51] J.P. Lange, A. Gutsze, H.G. Karge, J. Catal. 114 (1988) 136.
[52] A.V. Kucherov, A.A. Slinkin, Zeolites 7 (1987) 38.
[53] B. Wichterlova, J. Dedecek, A. Vondrova, J. Phys. Chem. 99 (1995) 1065.
[54] J. Dedecek, Z. Sobalik, Z. Tvaruzkova, D. Kaucky, B. Wichterlova, J. Phys. Chem. 99 (1995) 16327.
[55] D. Ma, X. Han, D. Zhou, Z. Yan, R. Fu, Y. Xu, X. Bao, H. Hu, S.C.F. Au-Yeung, Chemisty 8 (2002) 4557.
[56] W. Zhang, D. Ma, X. Han, X. Liu, X. Bao, X. Guo, X. Wang, J. Catal. 188 (1999) 393.